TITLE

Transcriptome analysis of left-right intrinsic laryngeal muscles shows divergent expression of genes associated with innervation.

AUTHORS

Angela M. Kemfack, BS[1]; Ignacio Hernández-Morato, PhD[1*]; Yalda Moayedi, PhD[1,2]; Michael J. Pitman, MD[1]

1. Department of Otolaryngology-Head & Neck Surgery, The Center for Voice and Swallowing, Columbia University College of Physicians and Surgeons, New York, NY

2. Department of Neurology, Columbia University College of Physicians and Surgeons, New York, NY

KEYWORDS

Laterality, innervation, laryngeal muscles, recurrent laryngeal nerve injury, neuroinflammation, vocal fold paralysis

FUNDING: This work was supported by the National Institutes of Health 1R01DC018060-1.

Correspondence regarding this manuscript may be addressed to:

Dr. Ignacio Hernández-Morato,

180 Fort Washington Ave, Harkness Pavilion 8-860, 8th Floor,

Columbia University Medical Center, NY 10032.

E-mail: ih2302@cumc.columbia.edu

ABSTRACT

Objectives/Hypothesis: Recurrent laryngeal nerve neuropathy diagnosed as idiopathic or due to short-term surgery-related intubation exhibits a higher incidence of left-sided paralysis. While this is often attributed to nerve length, it is hypothesized there are asymmetric differences in the expression of genes related to neuromuscular function that may impact reinnervation and contribute to this laterality phenomenon. To test this hypothesis, this study analyzes the transcriptome profiles of the intrinsic laryngeal muscles (ILMs), comparing gene expression in the left versus right, with particular attention to genetic pathways associated with neuromuscular function.

Study Design: Laboratory experiment.

Methods: High-quality RNA was extracted from the left and right sides of the rat posterior cricoarytenoid (PCA), lateral thyroarytenoid (LTA), and medial thyroarytenoid (MTA), respectively. After high-throughput RNA-Sequencing (RNA-Seq), 88 samples were organized into 12 datasets according to their age (P15/adult), sex (male/female), and muscle type (PCA/LTA/MTA). A comprehensive bioinformatics analysis was conducted to compare the left-right ILMs across different conditions.

Results: 774 differentially expressed genes (DEGs) were identified across the 12 experimental groups, revealing age, sex, and muscle-specific differences between the left versus right ILMs. Enrichment analysis of Gene Ontology (GO) and Kyoto Encyclopedia of Genes and Genomes (KEGG) pathways implicated several genes with a left-right laryngeal muscle asymmetry. These genes are associated with neurogenic and myogenic processes, immune/inflammatory response, and hormone control.

Conclusion: Clinically, recurrent laryngeal nerve neuropathy diagnosed as idiopathic or due to short-term surgery related intubation exhibits a higher incidence of left-sided paralysis. While this is often attributed to nerve length, it is hypothesized there are asymmetric differences in the

expression of genes related to neuromuscular function that may impact reinnervation and contribute to this laterality phenomenon. To test this hypothesis, this study analyzes the transcriptome profiles of the intrinsic laryngeal muscles (ILMs), comparing gene expression in the left versus right, with particular attention to genetic pathways associated with neuromuscular function.

Level of Evidence: N/A

LAY SUMMARY

Vocal fold paralysis is more common on the left. This study shows left versus right differences in gene expression related to innervation, suggesting the increased rate of left recurrent laryngeal nerve paralysis may be associated with genetic differences, not just nerve length.

KEY WORDS:

Intrinsic laryngeal muscles, laterality, nerve regeneration, differential gene expression, RNA-Seq, vocal fold paralysis

INTRODUCTION

Normal vocal fold function is necessary for the fundamental activities of daily life: eating, breathing, and speaking. Recurrent laryngeal nerve (RLN) injury results in vocal fold paralysis due to synkinetic reinnervation[1]. Vocal fold paralysis causes dysphagia and dysphonia, which leads to frustration, isolation, fear, lost worker productivity, and altered self-identity[2-5]. While current treatments have adequate results, they are suboptimal and disability claims are at rates similar to those of chronic diseases like congestive heart failure, chronic obstructive pulmonary disease, and severe depression[2, 3].

Efforts to restore normal vocal fold function focus on the guidance of reinnervating injured axons back to the correct laryngeal muscle to prevent synkinetic reinnervation and the resultant paralysis[1, 6]. Understanding the genes expressed by ILMs related to innervation and reinnervation in the healthy state and after RLN injury may identify high-value genes. These genes can be investigated as therapeutic targets for manipulation after nerve injury to guide axons to the appropriate muscle and restore normal vocal fold function.

Robust clinical evidence supports a greater incidence of left vocal fold paralysis versus right [7-15]. Sidedness of the paralysis has been hypothesized to result from the extended length of the left RLN for this reason. Further, its course through the thorax may also increase the risk of injury from thoracic disease and surgery compared to the right RLN[16]. Left RLN reinnervation is more demanding than on the right side because it requires an increased energy expenditure for protein translation and transport from the cell body to the nerve growth cone [17-20]. The intra-axonal transport hypothesis also implicates the reliance on rapid mitochondrial transport to areas along the axon of high energy demand[21, 22]. This phenomenon would make the more elongated left RLN more vulnerable to acute injury than the right.

Cases of idiopathic vocal fold paralysis and paralysis after short-term intubation for surgery also show similar discrepancies in lateral rates[23-26]. These are states where the RLN extension and trajectory should not impact the rate of injury. This persistent sidedness suggests intrinsic neuromuscular differences between the left and right sides may also play a role in the frequency of paralysis[26]. In addition, previous findings indicate that intrinsic laryngeal muscles (ILM) exhibit different fiber-type compositions on the left versus the right side in equines[10]. Considering that targeted axon outgrowth to the ILMs requires a dialogue between the motoneurons and muscle fibers, an analysis of ILM gene expression may provide insights into the asymmetry of the larynx. These changes in gene expression could also explain the sidedness of vocal fold paralysis[27]. Moreover, organ asymmetry has already been identified in the diaphragm muscles and the phrenic nerves that innervate them[28]. If intrinsic neuromuscular differences in the larynx (aside from length) influence disparities in reinnervation between sides, these differences may be exploited as therapeutic targets.

The present work aims to investigate inherent neuromuscular differences by testing the hypothesis that, in uninjured laryngeal muscles, there are asymmetric discrepancies in gene expression related to neuromuscular function. Such genes are likely to contribute to the disparity in the incidence of left versus right vocal fold paralysis and warrant further investigation. This study uses recently described techniques to evaluate differences in the transcriptome between the respective left-right posterior cricoarytenoid (PCA), lateral (LTA), and medial thyroarytenoid (MTA) muscles_in an uninjured rat model to establish the baseline of gene expression in the healthy animal[29].

MATERIALS AND METHODS

Rats and Housing

A total of 82 Sprague Dawley rats were used in this study and distributed in 12 groups according to age (adult and P15), sex (male and female), and type of muscle (PCA, LTA, and MTA). A schematic representation of the experimental design is illustrated in Figure 1. This study was performed in compliance with the Public Health Service Policy on Humane Care and Use of Laboratory Animals, the National Institutes of Health Guide for the Care and Use of Laboratory Animals, the Animal Welfare Act (7 U.S.C. et seq.), and the ARRIVE guidelines. The Institutional Animal Care and Use Committee of Columbia University Medical Center approved the animal use protocol.

Surgical Procedure and Tissue Processing

All rats were euthanized via an overdose of ketamine and xylazine before the larynx was dissected out. ILM isolation for RNA-Seq was performed as previously described [29]. Harvested larynxes were stabilized by briefly rinsing in 2 mL of RNA*later* (catalog #AM7021, Invitrogen, Waltham, MA, U.S.A.) prior to dissection of the muscle bellies using a Leica S8 APO compound microscope (Leica Microsystems, Buffalo Grove, IL). With micro-forceps and micro-scissors, the left and right PCA, LTA, and MTA were carefully excised and stored overnight at 4 C° in 1 mL RNA*later*. The next day, excess stabilizing reagent was removed and the muscle bellies were placed into BioMasher III (Nippi, Inc., Japan) homogenization tubes according to the age, sex, and muscle type (Figure 1). Samples were physically disrupted in liquid nitrogen before adding lysis buffer from the Aurum Total RNA Mini Kit (catalog #732-6820, Bio-Rad, Hercules, CA, U.S.A.). Further homogenization was conducted using a

TissueRuptor II (catalog #9002755, Qiagen, MD). All proceeding steps were according to the commercial RNA isolation protocol. Total RNA was measured using a micro-volume spectrophotometer NanoDrop ONE (catalog #ND-ONE-W, Thermofisher, Wilmington, DE). Agilent RNA 6000 Pico Kit (Eukaryote Total RNA Pico, Agilent Technologies, Santa Clara, CA, U.S.A.) and Agilent 2100 bioanalyzer (Agilent Technologies, Santa Clara, CA, U.S.A.) were used to evaluate the RIN. The recovered RNA used in the subsequent sequencing steps reached a RIN value of 7.9 ± 0.4 (N = 90).

Library Preparation and RNA Sequencing

The following RNA-Sequencing procedures were performed using the Illumina NextSeq 500 (Illumina Inc., San Diego, CA, U.S.A.) desktop sequencer at the Columbia University Genome Center. Standard analytics were obtained by first using a poly-A pull-down method to enrich mRNA from the total RNA within the sample. Library construction then proceeded using TruSeq chemistry and was sequenced by the NovaSeq 6000 platform (Illumina, Inc). Samples were multiplexed in each lane and pseudo-aligned to a kallisto (0.44.0) index created from human (GRCh38) and mouse (GRCm38) transcriptomes. After quality control steps, the pseudo-aligned reads were mapped to the annotated *Rattus norvegicus* genome assembly Ensembl database.

Measured Expression Analysis

Differential gene expression analysis in the left versus the right respective ILM was performed through the EdgeR Bioconductor Package 3.32. Sample counts were normalized with qsmooth. Limma-zoom was used to evaluate the sample weights and downweigh the effect of sample outliers. A comprehensive list of differentially expressed genes (DEGs) was generated under

three different conditions in the left versus the right comparison. 88 samples, not including the controls, were dichotomized into “left" vs. “right” groups according to the muscle, age, and gender of the rat. The total number of DEGs exhibited using False Discovery Rate (FDR)<0.05 and log fold change >|0.6| across all rat cohorts is displayed in **Table 1**. Raw data can be found in the Gene Expression Omnibus (https://www.ncbi.nlm.nih.gov/geo/query/acc.cgi?acc=GSM6703793).

iPathwayGuide Analysis

Advaita Bioinformatics iPathwayGuide analysis identified significant genes based on a log fold change of expression with an absolute value of at least 0.6 and a 0.05 threshold for the p-value. Data were analyzed in the context of pathways obtained from the Kyoto Encyclopedia of Genes and Genomes (KEGG) database (Release 100.0+/11-12, Nov 21). Gene Ontologies were obtained from the Gene Ontology Consortium Database. Impact analyses for pathway analysis were evaluated by over-representation of differentially expressed genes in a given pathway and the perturbation of that pathway computed by propagating the measured expression changes across the pathway topology.

RESULTS

Sequencing of the transcriptome across the ninety ILM samples resulted in a mean of 32.9 million mapped reads and a 79.1% mean mapping ratio, with no less than 70% sequence alignment in any sample. Principal component (PC) analysis by experimental condition (i.e., sex, age, ILM) indicated that PC1 and PC2 accounted for 98% variance. Samples were normalized,

then, using a mean-variance trend into precision weights, the effects of sample outliers were downweighed. Further quality control measures validated the differential control analysis.

Overview of Differential Gene Analysis

Differential expression analysis confirmed asymmetric gene transcriptome profiles between the left-right ILMs according to age, sex, and distinctive muscle (Table 1, Figure 2). Across all PCA and LTA experimental groups, DEGs showed only lower expression (downregulation) on the left versus the right. In contrast, at least 63% of DEGs in the P15 and 95% in the adult MTA were higher (upregulated) on the left relative to the right side (Table 1, Figure 2A). Overall, adult males exhibited the most substantial number of DEGs in each muscle type, with comparatively few DEGs identified in adult females or at P15 in either sex (Figure 2B). Excluding the MTA, which showed overlapping significant genes, DEGs varied per experimental condition (Figure 2C). Generally, the function of the DEGs per each experimental condition fell under two broad categories: neurophysiological and myogenic factors (Table 1). Gene Ontology (GO) and KEGG Pathways also evidenced asymmetric differences related to inflammatory/immune response and hormonal control. These findings varied according to age, sex, and distinctive ILM.

PCA

Across the global data, the PCA showed the fewest DEGs of any comparison (Figure 2B). GO Classifications and KEGG Pathways in the left-right adult male PCA indicated that DEGs were highly associated with inflammatory/immune response mechanisms, hormonal control, and neurophysiological processes (Figure 3A, C). Common KEGG pathways between the adult male PCA and MTA datasets showed considerable enrichment of DEGs involved in inflammatory/

immune signaling (Figure 3C). The top pathways of the adult male included ‘antigen processing and presentation’ in addition to ‘Th1 and Th2 cell differentiation’, which are established inflammatory/immune response mechanisms. Interestingly, differential expression analysis in the left-right adult male PCA did not implicate the involvement of myogenic processes in the PCA asymmetry. The adult female PCA only exhibited differential expression of a single mitochondrial iron ion transporter gene, Slc25a37, between sides and thus was not amenable to further GO or biological pathway analysis (Figure 2B).

LTA

The adult male LTA dataset was the only condition to exhibit significant differential gene expression in the left compared to the right. GO and KEGG pathway enrichment analysis indicated that DEGs represented in the adult male LTA were highly associated with neurophysiological, myogenic, inflammatory, and hormonal regulation (Figure 4). Specifically, top GOs included the ‘semaphorin-plexin signaling pathway’, a hallmark of axon guidance, and the ‘postsynaptic neurotransmitter receptor cycle’ (Figure 4A). Top myogenic factors and inflammatory response included ‘satellite cell activation involved in skeletal muscle regeneration’ and ‘negative regulation of necrotic cell death’, respectively (Figure 4A). Top KEGG Pathways demonstrated highly associated DEGs involved in inflammatory/immune response, such as the ‘IL-17 signaling pathway’, and neurophysiological processes, such as the ‘calcium signaling pathway’ (Figure 4B).

MTA

Overall, the MTA showed the most DEGs of any condition (Figure 2A). DEGs in this muscle group were identified across sexes in both the adult and P15 datasets, although the high number of DEGs intersecting between the adult male and female MTA is most likely attributable to residual mucosa surrounding the muscle during dissection. GO Classification in the adult male and female MTA datasets demonstrated the enrichment of inflammatory, neurophysiological, myogenic, and hormonal processes; however, no common pathways that regulate hormonal control were found between the adult male and female datasets (Figure 5A, B, D). In contrast, similar KEGG Pathways that direct hormonal control were identified between the adult and P15 male MTA (Figure 5D, E). Top GO Classifications in the P15 male MTA included relevant myogenic and neurophysiological factors, such as 'regulation of muscle adaptation' and 'inhibitory chemical synaptic transmission in response to denervation'. Relevant neurological pathways across the adult male, adult female, and P15 male MTA included 'neuroactive-ligand receptor interaction' and 'adrenergic signaling in cardiomyocytes', which may be similar to pathways in striated muscles that are less characterized. (Figure 5C).

Age and sex-specific differences

P15 muscles generally demonstrated less significant left-right differences in gene expression compared to the adult conditions (Table 1). The PCA and LTA showed no lateral differences at P15 (Figure 4). Markers of inflammatory regulation showed marginal differential expression in P15 rats compared to adults, which demonstrated the involvement of immune response mechanisms in every adult experimental condition (Figures 3B, 5C, and 5E). Left-right differences corresponding to sex were primarily distinguished in the adult male MTA, given the lack of significant DEGs in the female PCA and LTA muscles. Differential expression analysis

consistently exhibited enriched pathways and gene ontologies involved in hormonal control (in particular via thyroid hormone regulation and insulin signaling) across all male datasets (Figures 3 to 5). Common KEGG pathways across the adult male PCA, LTA, and MTA were limited to inflammatory processes, while the only similarity between the adult female PCA and MTA was the annotation of 'iron ion import across plasma membrane' (Figure 6).

DISCUSSION

The left-right ILM transcriptome profile indicates that laterality is influenced by age, sex, and tissue-specific differences. Reviewing the KEGG Pathways and GO Classifications of DEGs across all experimental conditions allows for identifying genes that may contribute to the intrinsic laterality of laryngeal innervation and reinnervation. The results of this study indicated differences in transcriptional regulation between the left-right abductor and adductor muscles. Of the global female and male conditions only 3.0% and 4.8% of left versus right DEGs were found in the abductor muscle compared to the adductor, respectively. Despite having no overlap of DEGs across the left-right PCA, LTA, and MTA muscles, similar regulatory mechanisms between the arytenoid adductors suggest diverse and systematic causes of laterality in the healthy state (Figure 2B). These uncharacterized cellular interactions will require further functional assays to distinguish the specific role of the significant genes involved.

Differential expression analysis demonstrates two general influences regulating the laterality of ILM innervation in uninjured tissue: myogenic and neurogenic factors. For instance, the most common pathways identified across the global data included 'axon guidance' and the 'calcium signaling pathway'. The GO and KEGG pathways of the implicated DEGs also suggest they exert their influence via inflammatory responses and hormonal control (Figures 3-5). This

finding corresponds with the reliance on immune response and hormone signals to promote peripheral nerve regeneration after injury. In the former case, functional recovery of the peripheral nerve tissue is facilitated by inflammatory-related genes in an innate immune response[30]. Neurotrophic and guidance factors are upregulated during nerve regeneration, while myelin-associated inhibitors are cleared to promote distal neurite outgrowth to the original targets[31]. In the latter event, recent studies have evidenced hormonal control as an essential component of muscle reinnervation after nerve injury. Of relevance, growth hormone treatment in the rat forelimb was associated with significantly attenuated muscle atrophy and enhanced nerve regeneration, muscle reinnervation, and motor function[32]. Thyroid hormone and its receptors, localized in Schwann cells, are also critical for promoting nerve[33]. The absence of DEGs related to inflammation in P15 muscles may reflect the development of the immune system between P15 and adulthood[34]. Indeed, this phenomenon would agree with age-dependent and sex-related studies concerning musculature hormone control, though further analysis is needed to justify this association[11, 13, 35-38].

Possible limitations of this study are related to the (1) testing of ILM via bulk rather than single-cell RNA-seq, (2) the risk of containing fibers from adjacent muscle or mucosa during microdissection of the laryngeal muscles, and (3) the tissue pooling size. Differences in DEGs with respect to laterality were more strongly detected between the gene sets rather than at the level of the individual genes. Identifying subtle differences in gene expression will require validation of putative targets via functional assays, such as RT-PCR. Inaccurate muscle dissection could conflate the sequencing results with small amounts of alternative muscle or mucosa contaminating a sample. While confident in our microsurgical techniques, this study recognizes the inherent difficulty in isolating the left from the right PCA at the midline raphe and

removing all remnants of mucosa from the left and right MTA. Normalization and downweighing of sample outliers were performed during the quality control step to minimize the impact of this issue. The pooling strategy implemented to systematically obtain sufficient high-quality RNA required muscle aggregation from three distinct rats. Due to the influence of multiple transcripts per sample, sequencing results could be perturbed by the overrepresentation of one transcriptome profile over another. Pooling bias for RNA can be reduced by increasing the number of biological replicates or increasing the pooled sample size to at least eight tissues to reduce the false discovery rate [29, 39, 40].

CONCLUSION

Differential expression analysis of the left-right ILM transcriptome identified age, sex, and muscle-dependent differences in the healthy state. Several common processes implicated in the laterality of ILM gene expression have been shown to influence innervation, These factors include neurophysiological and myogenic processes, inflammatory response, and hormonal control. The genes of interest identified in this study will be evaluated after RLN injury and in models of reinnervation to study their impact on RLN reinnervation.

REFERENCES

1. Crumley, R.L., *Laryngeal synkinesis revisited.* Ann Otol Rhinol Laryngol, 2000. **109**(4): p. 365-71.
2. Cohen, S.M., W.D. Dupont, and M.S. Courey, *Quality-of-life impact of non-neoplastic voice disorders: a meta-analysis.* Ann Otol Rhinol Laryngol, 2006. **115**(2): p. 128-34.
3. Cohen, S.M., et al., *The impact of laryngeal disorders on work-related dysfunction.* The Laryngoscope, 2012. **122**(7): p. 1589-1594.
4. Francis, D.O., et al., *Life Experience of Patients With Unilateral Vocal Fold Paralysis.* JAMA Otolaryngol Head Neck Surg, 2018. **144**(5): p. 433-439.
5. Meyer, T.K., A. Hu, and A.D. Hillel, *Voice disorders in the workplace: Productivity in spasmodic dysphonia and the impact of botulinum toxin.* The Laryngoscope, 2013. **123**(S6): p. S1-S14.
6. Hernandez-Morato, I., S. Sharma, and M.J. Pitman, *Changes in neurotrophic factors of adult rat laryngeal muscles during nerve regeneration.* Neuroscience, 2016. **333**: p. 44-53.
7. Seyed Toutounchi, S.J., et al., *Vocal cord paralysis and its etiologies: a prospective study.* J Cardiovasc Thorac Res, 2014. **6**(1): p. 47-50.
8. Özbal Koç, A.E., et al., *Vocal cord paralysis: What matters between idiopathic and non-idiopathic cases?* Kulak Burun Bogaz Ihtis Derg, 2016. **26**(4): p. 228-33.
9. Politano, S., et al., *Yield of Imaging to Evaluate Unilateral Vocal Fold Paralysis of Unknown Etiology.* The Laryngoscope, 2021. **131**(8): p. 1840-1844.
10. Rhee, H.S., et al., *Immunohistochemical analysis of laryngeal muscles in normal horses and horses with subclinical recurrent laryngeal neuropathy.* J Histochem Cytochem, 2009. **57**(8): p. 787-800.
11. Yamada, M., M. Hirano, and H. Ohkubo, *Recurrent laryngeal nerve paralysis. A 10-year review of 564 patients.* Auris Nasus Larynx, 1983. **10 Suppl**: p. S1-15.
12. Johansson, S., P.-O. Löfroth, and J. Denekamp, *Left sided vocal cord paralysis: a newly recognized late complication of mediastinal irradiation.* Radiotherapy and Oncology, 2001. **58**(3): p. 287-294.
13. Ahmad, S., A. Muzamil, and M. Lateef, *A Study of incidence and etiopathology of vocal cord paralysis.* Indian J Otolaryngol Head Neck Surg, 2002. **54**(4): p. 294-6.
14. Leder, S.B. and D.A. Ross, *Incidence of Vocal Fold Immobility in Patients with Dysphagia.* Dysphagia, 2005. **20**(2): p. 163-167.
15. Singh, J.M., R. Wang, and G. Kwartowitz, *Unilateral Vocal Fold Paralysis*, in *StatPearls*. 2022, StatPearls Publishing

Copyright © 2022, StatPearls Publishing LLC.: Treasure Island (FL).

16. Singh, J.M., R. Wang, and G. Kwartowitz, *Unilateral Vocal Fold Paralysis*, in *StatPearls*. 2023, StatPearls Publishing

Copyright © 2023, StatPearls Publishing LLC.: Treasure Island (FL).

17. Maday, S., et al., *Axonal transport: cargo-specific mechanisms of motility and regulation.* Neuron, 2014. **84**(2): p. 292-309.
18. Rishal, I. and M. Fainzilber, *Axon–soma communication in neuronal injury.* Nature Reviews Neuroscience, 2014. **15**(1): p. 32-42.
19. Hanz, S., et al., *Axoplasmic importins enable retrograde injury signaling in lesioned nerve.* Neuron, 2003. **40**(6): p. 1095-104.

20. Guedes-Dias, P. and E.L.F. Holzbaur, *Axonal transport: Driving synaptic function.* Science (New York, N.Y.), 2019. **366**(6462): p. eaaw9997.
21. Ginsberg, L., *Acute and chronic neuropathies.* Medicine (Abingdon), 2020. **48**(9): p. 612-618.
22. English, K. and M.C. Barton, *HDAC6: A Key Link Between Mitochondria and Development of Peripheral Neuropathy.* Front Mol Neurosci, 2021. **14**: p. 684714.
23. Jacks, A., et al., *Computed Tomography Measurements in Assessment of Idiopathic Vocal Fold Paralysis.* J Voice, 2023. **37**(2): p. 289.e15-289.e21.
24. Kikura, M., et al., *[Vocal cord paralysis associated with tracheal intubation: incidence, risk analysis, and classification of severity].* Masui, 2015. **64**(1): p. 57-9.
25. Geng, Z.Y., W.H. Gao, and D.X. Wang, *[Clinical outcomes of vocal fold immobility after tracheal intubation].* Beijing Da Xue Xue Bao Yi Xue Ban, 2020. **53**(2): p. 337-340.
26. Aaron, O. and J.P. Michael, *Intrinsic Susceptibility Of The Left Vs Right Recurrent Laryngeal Nerve To Paralysis: A Systematic Review.* medRxiv, 2023: p. 2023.08.09.23293889.
27. Lepore, E., et al., *Neuromuscular Junction as an Entity of Nerve-Muscle Communication.* Cells, 2019. **8**(8).
28. Charoy, C., et al., *Genetic specification of left-right asymmetry in the diaphragm muscles and their motor innervation.* Elife, 2017. **6**.
29. Kemfack, A.M., et al., *An optimized method for high-quality RNA extraction from distinctive intrinsic laryngeal muscles in the rat model.* Scientific Reports, 2022. **12**(1): p. 21665.
30. Büttner, R., et al., *Inflammaging impairs peripheral nerve maintenance and regeneration.* Aging Cell, 2018. **17**(6): p. e12833.
31. Rotshenker, S., *Wallerian degeneration: the innate-immune response to traumatic nerve injury.* Journal of Neuroinflammation, 2011. **8**(1): p. 109.
32. Lopez, J., et al., *Growth Hormone Improves Nerve Regeneration, Muscle Re-innervation, and Functional Outcomes After Chronic Denervation Injury.* Sci Rep, 2019. **9**(1): p. 3117.
33. Papakostas, I.D. and G.A. Macheras, *Thyroid hormones and peripheral nerve regeneration.* J Thyroid Res, 2013. **2013**: p. 648395.
34. Simon, A.K., G.A. Hollander, and A. McMichael, *Evolution of the immune system in humans from infancy to old age.* Proc Biol Sci, 2015. **282**(1821): p. 20143085.
35. Parikh, S.R., *Pediatric unilateral vocal fold immobility.* Otolaryngologic Clinics of North America, 2004. **37**(1): p. 203-215.
36. Rong, X., et al., *FRMPD1 activates the Hippo pathway via interaction with WWC3 to suppress the proliferation and invasiveness of lung cancer cells.* Cancer management and research, 2019. **11**: p. 3395-3410.
37. Coletti, C., et al., *Exercise-mediated reinnervation of skeletal muscle in elderly people: An update.* Eur J Transl Myol, 2022. **32**(1).
38. Piasecki, M., et al., *Age-dependent motor unit remodelling in human limb muscles.* Biogerontology, 2016. **17**(3): p. 485-96.
39. Rajkumar, A.P., et al., *Experimental validation of methods for differential gene expression analysis and sample pooling in RNA-seq.* BMC Genomics, 2015. **16**(1): p. 548.

40. Takele Assefa, A., J. Vandesompele, and O. Thas, *On the utility of RNA sample pooling to optimize cost and statistical power in RNA sequencing experiments.* BMC Genomics, 2020. **21**(1): p. 312.

Figure Legends

Figure 1. A schematic diagram illustrating the experimental design for high-throughput RNA-Sequencing (RNA-Seq) of the distinctive intrinsic laryngeal muscles.

Figure 2. Global differential expression analysis summary comparing gene regulation in the left versus right ILMs. (A) Volcano Plot showing statistically significant genes and their fold change in gene expression across the P15 and adult PCA, LTA, and MTA muscles in both male and female rats. Downregulated differentially expressed genes (DEGs) on the left compared to the right ILMs are represented in blue, while upregulated DEGs are depicted in red. DEGs that were not significant (p-value > 0.05; log fold change > |0.6|) are shown in gray. (B) Number of DEGs in the left compared to the right across each experimental condition. (C) Venn diagram indicating the number of genes that overlapped across all experimental conditions. Common DEGs across the global data only intersected two datasets in the MTA muscle; specifically, the adult male and female MTA. Venn diagram created using Venny (Oliveros, J.C. (2007-205) Venny. An interactive tool for comparing list with Venn's diagrams. https://bioinfogp.cnb.csic.es/tools/venny/index.html)

Figure 3. Key Gene Ontology and KEGG pathways enriched in the PCA muscle. (A) Top Gene Ontologies (GOs) enriched in the adult male left vs. right PCA muscle are classified by inflammatory, hormonal, and neurogenic sub-types in order of statistical significance. (B) Top Gene Ontologies (GOs) enriched in the P15 female left vs. right PCA muscle are classified by neurogenic, myogenic, and hormonal sub-types in order of statistical significance. (A-B) Biological processes are shown in green bars; molecular functions are represented in red bars, and cellular components are depicted in yellow bars. (C) Common KEGG pathways enriched in the left-right PCA were only identified between the adult male PCA and adult male MTA datasets. Inflammatory, hormonal, and neurogenic sub-types are represented by statistical significance. Biological pathways enriched in the adult male PCA dataset are shown as blue bars and those of the adult male MTA dataset are depicted by dark blue bars.

Figure 4. Key Gene Ontology and KEGG pathways enriched in the LTA muscle. (A) Top Gene Ontologies (GOs) enriched in the adult male left vs. right LTA muscle are classified by neurogenic, inflammatory, hormonal, and myogenic sub-types in order of statistical significance. Biological processes are shown in green bars; molecular functions are represented in red bars, and cellular components are depicted in yellow bars. (B) Common KEGG pathways enriched in the left-right LTA were only identified between the adult male LTA and the adult male MTA datasets. Inflammatory, neurogenic, myogenic, and hormonal sub-types are represented by statistical significance. Biological pathways enriched in the adult male LTA dataset are shown as blue bars and those of the adult male MTA dataset are depicted by dark blue bars.

Figure 5. Key Gene Ontology and KEGG pathways enriched in the MTA muscle. (A) Top Gene Ontologies (GOs) enriched in the adult male left vs. right MTA are classified by inflammatory, hormonal, neurogenic, and myogenic factors in order of statistical significance. (B) Top Gene Ontologies (GOs) enriched in the adult female left vs. right MTA are classified by myogenic, neurogenic, hormonal, and inflammatory factors in order of statistical significance. (C) Top Gene Ontologies (GOs) enriched in the P15 male left vs. right MTA muscle are classified by

myogenic, hormonal, and neurogenic sub-types in order of statistical significance. (A-C) Biological processes are shown in green bars; molecular functions are represented in red bars, and cellular components are depicted in yellow bars. (D-E) Common KEGG pathways enriched in the left-right adult male MTA intersected all other adult male datasets in addition to the adult female MTA and P15 male datasets. (D) Neurogenic, myogenic, and inflammatory sub-types are represented by statistical significance. Biological pathways enriched in the adult female MTA dataset are shown as blue bars and those of the adult male MTA dataset are depicted by dark blue bars. (E) Neurogenic, myogenic, hormonal, and inflammatory sub-types are represented by statistical significance. Biological pathways enriched in the P15 male MTA dataset are shown as blue bars and those of the adult male MTA dataset are depicted by dark blue bars.

Figure 6. Common KEGG pathways enriched across the PCA, LTA, and MTA muscles. (A) Enriched biological pathways that intersect all laryngeal muscle types were found in the adult male datasets. The adult male PCA, LTA, and MTA datasets only showed an association with pathways involved in the inflammatory response.

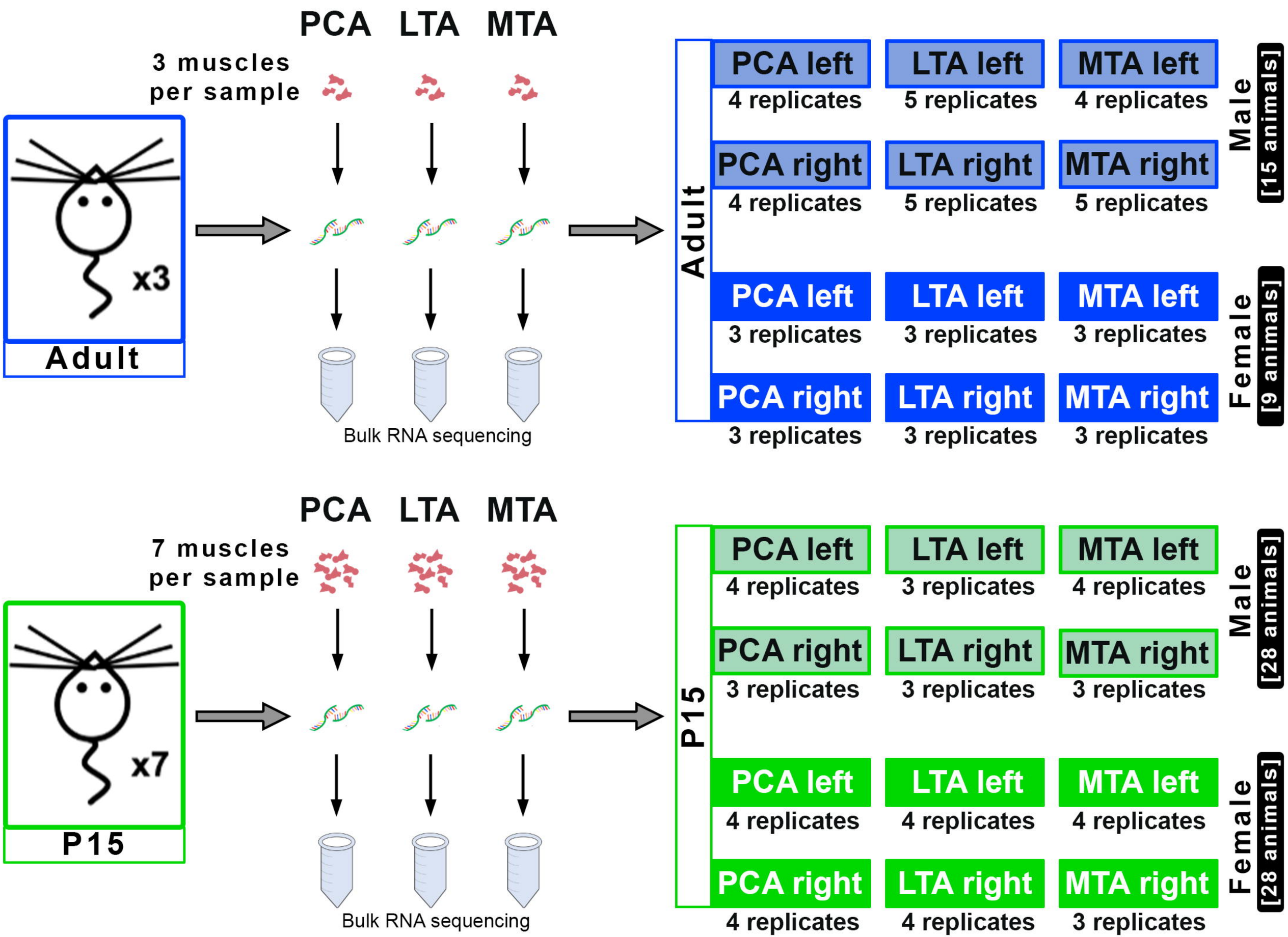

(+2 control animals)

Total = 82 animals

A

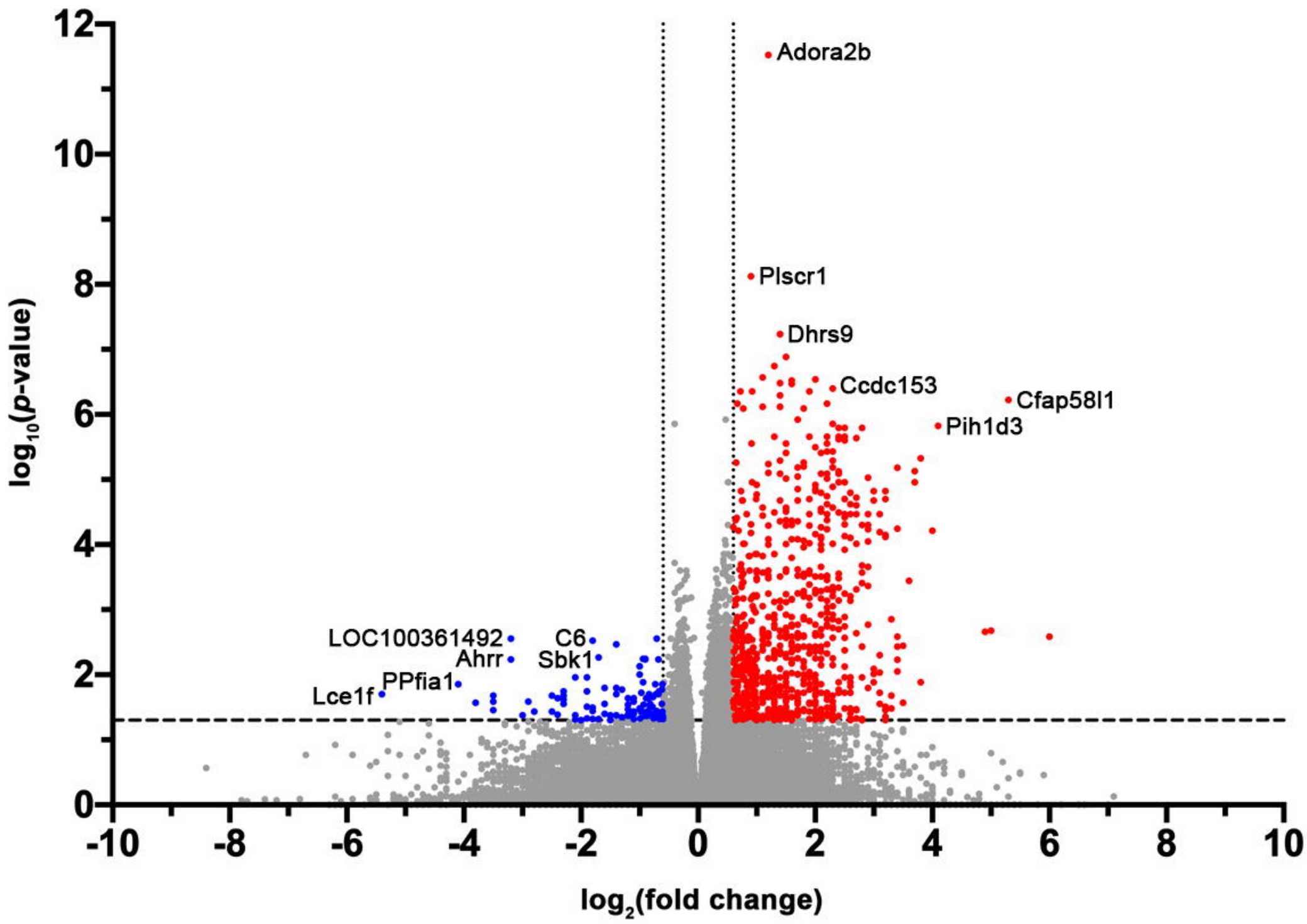
LEFT ILM VS. RIGHT ILM
log10(p-value)
log2(fold change)
Adora2b
Plscr1
Dhrs9
Ccdc153
Cfap58l1
Pih1d3
LOC100361492
C6
Ahrr
Sbk1
PPfia1
Lce1f

B

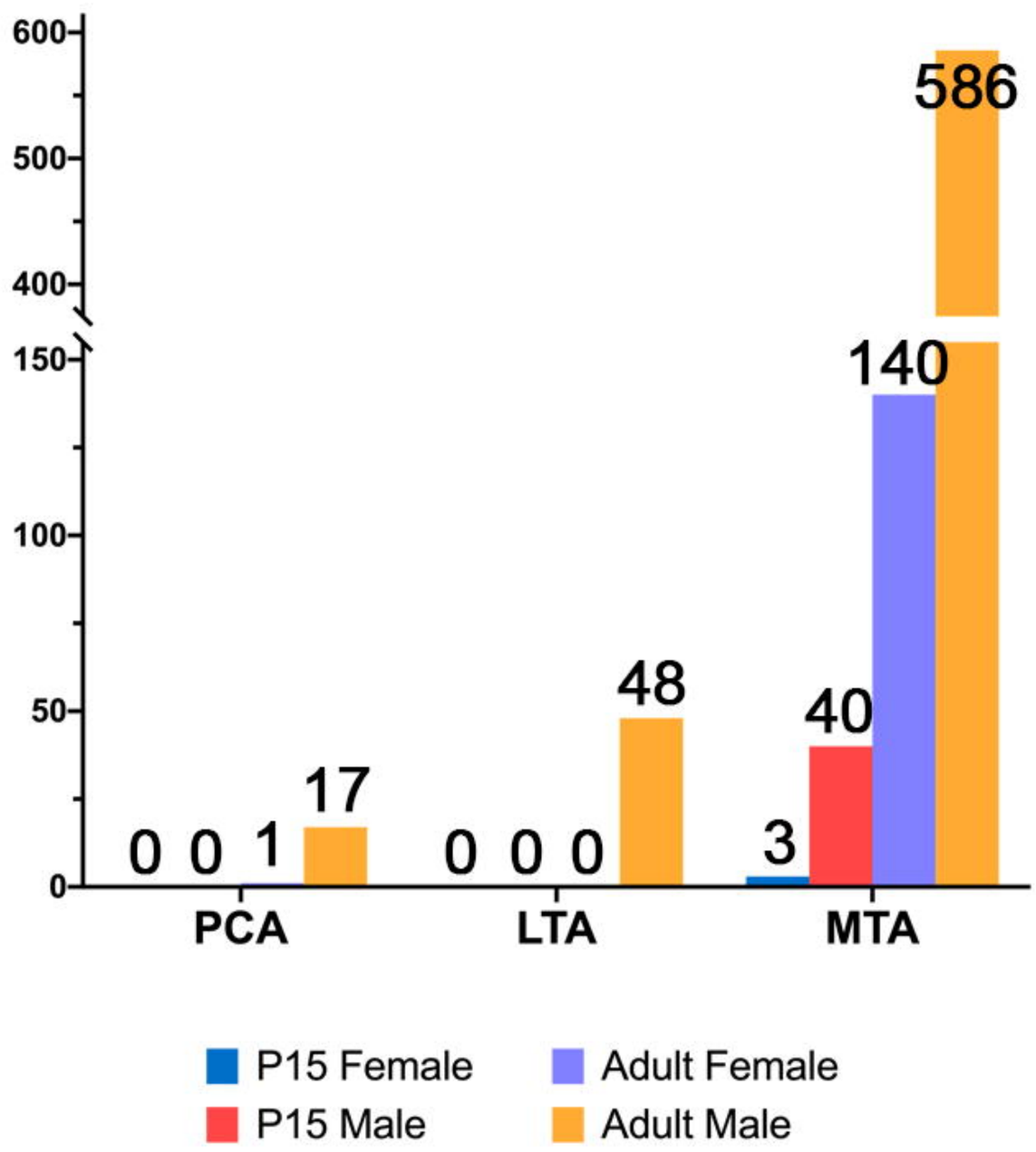
GENES PER EXPERIMENTAL CONDITION
586
140
48
40
17
0 0 1
0 0 0
3
PCA
LTA
MTA
P15 Female
P15 Male
Adult Female
Adult Male

C

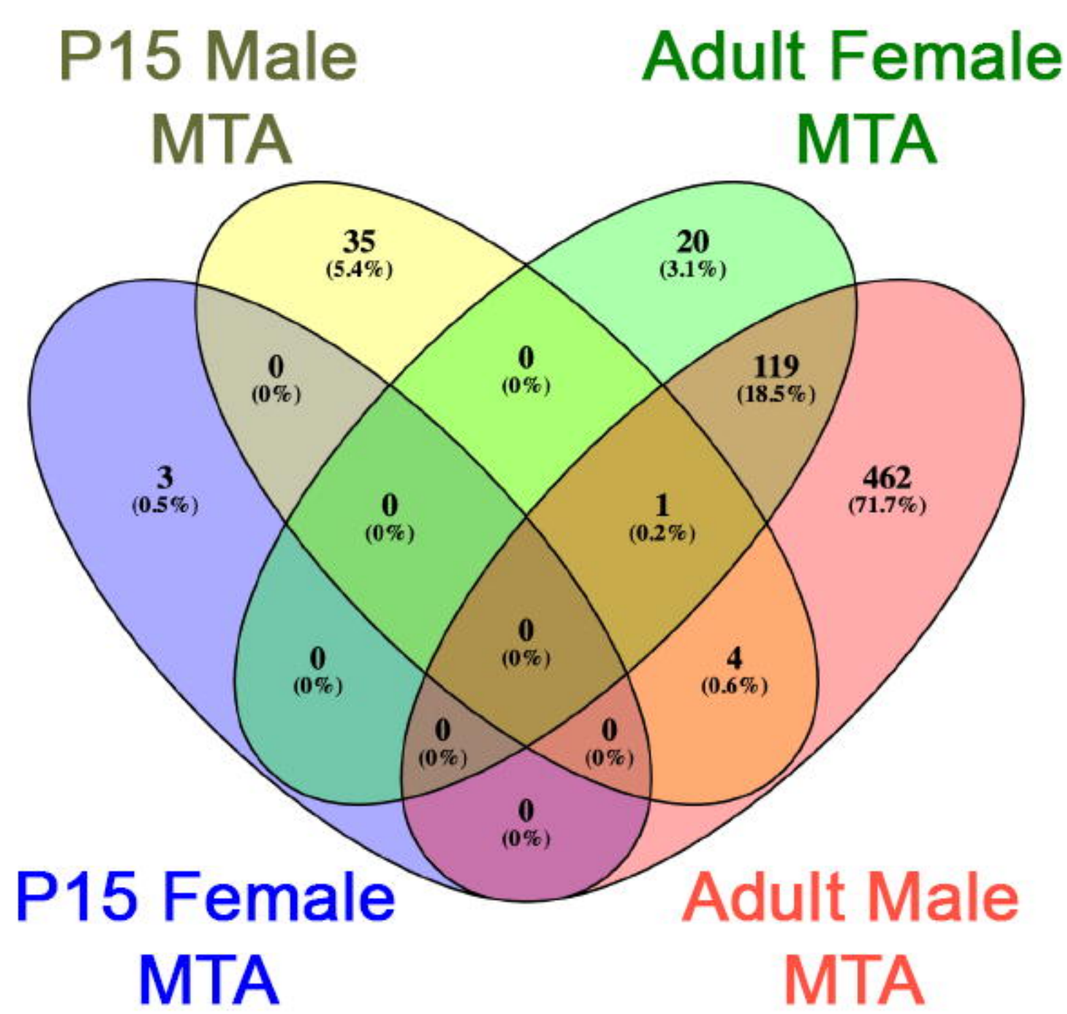
COMMON DIFFERENTIALLY EXPRESSED GENES
P15 Male MTA
Adult Female MTA
P15 Female MTA
Adult Male MTA
35 (5.4%)
20 (3.1%)
0 (0%)
0 (0%)
119 (18.5%)
3 (0.5%)
0 (0%)
1 (0.2%)
462 (71.7%)
0 (0%)
0 (0%)
4 (0.6%)
0 (0%)
0 (0%)
0 (0%)

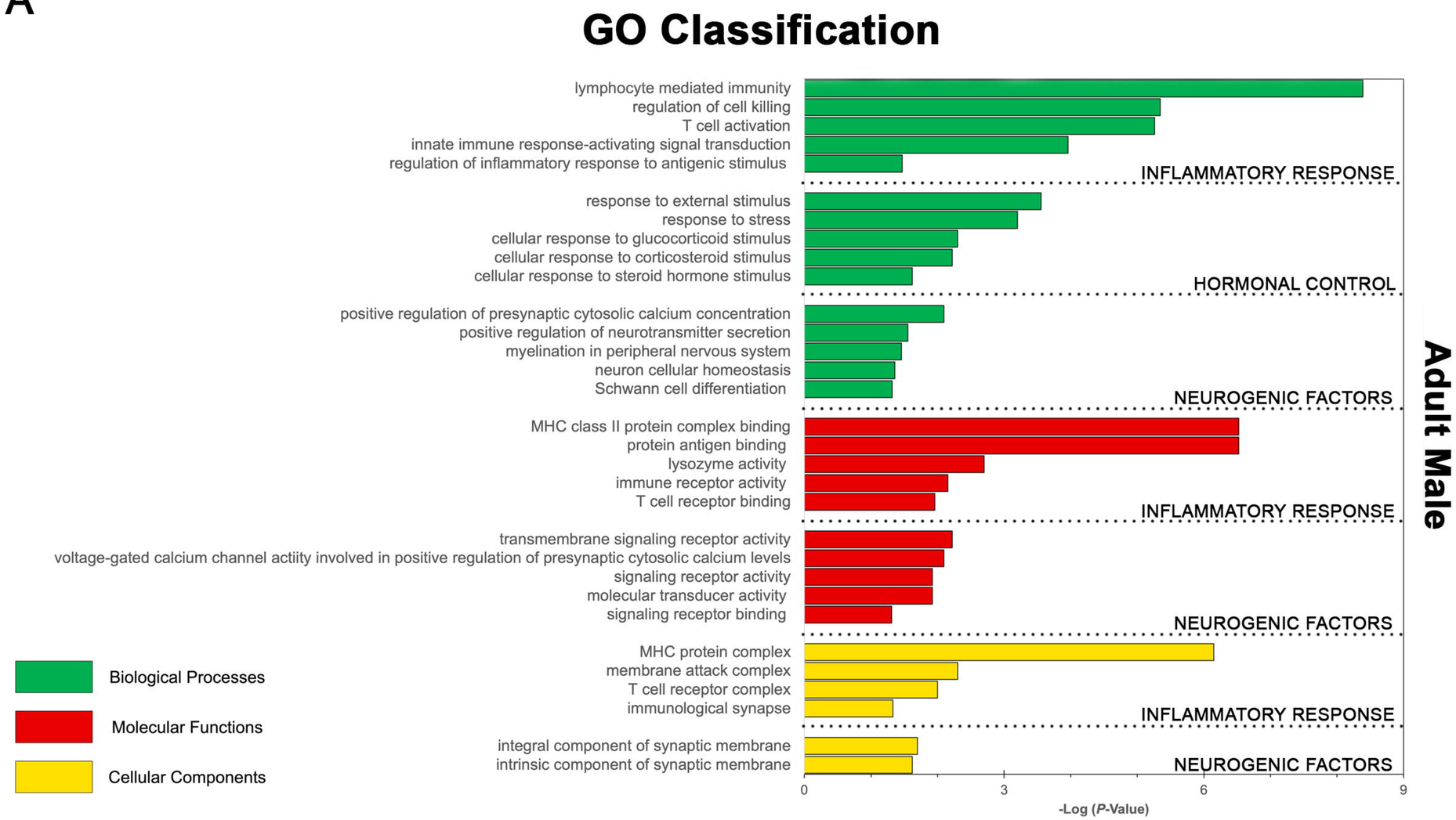
A
GO Classification
lymphocyte mediated immunity
regulation of cell killing
T cell activation
innate immune response-activating signal transduction
regulation of inflammatory response to antigenic stimulus
INFLAMMATORY RESPONSE
response to external stimulus
response to stress
cellular response to glucocorticoid stimulus
cellular response to corticosteroid stimulus
cellular response to steroid hormone stimulus
HORMONAL CONTROL
positive regulation of presynaptic cytosolic calcium concentration
positive regulation of neurotransmitter secretion
myelination in peripheral nervous system
neuron cellular homeostasis
Schwann cell differentiation
NEUROGENIC FACTORS
MHC class II protein complex binding
protein antigen binding
lysozyme activity
immune receptor activity
T cell receptor binding
INFLAMMATORY RESPONSE
transmembrane signaling receptor activity
voltage-gated calcium channel actiity involved in positive regulation of presynaptic cytosolic calcium levels
signaling receptor activity
molecular transducer activity
signaling receptor binding
NEUROGENIC FACTORS
MHC protein complex
membrane attack complex
T cell receptor complex
immunological synapse
INFLAMMATORY RESPONSE
integral component of synaptic membrane
intrinsic component of synaptic membrane
NEUROGENIC FACTORS
0
3
6
9
-Log (P-Value)
Adult Male
Biological Processes
Molecular Functions
Cellular Components
B
Common KEGG Pathways
Asthma
Systemic lupus erythematosus
Graft-versus-host-disease
Antigen processing and presentation
0.069
Intestinal immune network for IgA production
Inflammatory bowel disease
Rheumatoid arthritis
Th1 and Th2 cell differentiation
Human T-cell leukemia virus1 infection
Corona-virus disease COVID-19
0.027
Complement or coagulation cascades
Natural killer cell mediated cytotoxicity
T cell receptor signaling pathway
Fc gamma R-mediated phagocytosis
Cytokine-cytokine receptor interaction
INFLAMMATORY RESPONSE
Type 1 diabetes mellitus
Autoimmune thyroid disease
HORMONAL CONTROL
Retrograde endocannabinoid signaling
Neuroactive-ligand receptor interaction
NEUROGENIC FACTORS
6
4
2
0
-Log (P-Value)
Adult Male PCA
Adult Male MTA

PCA

A

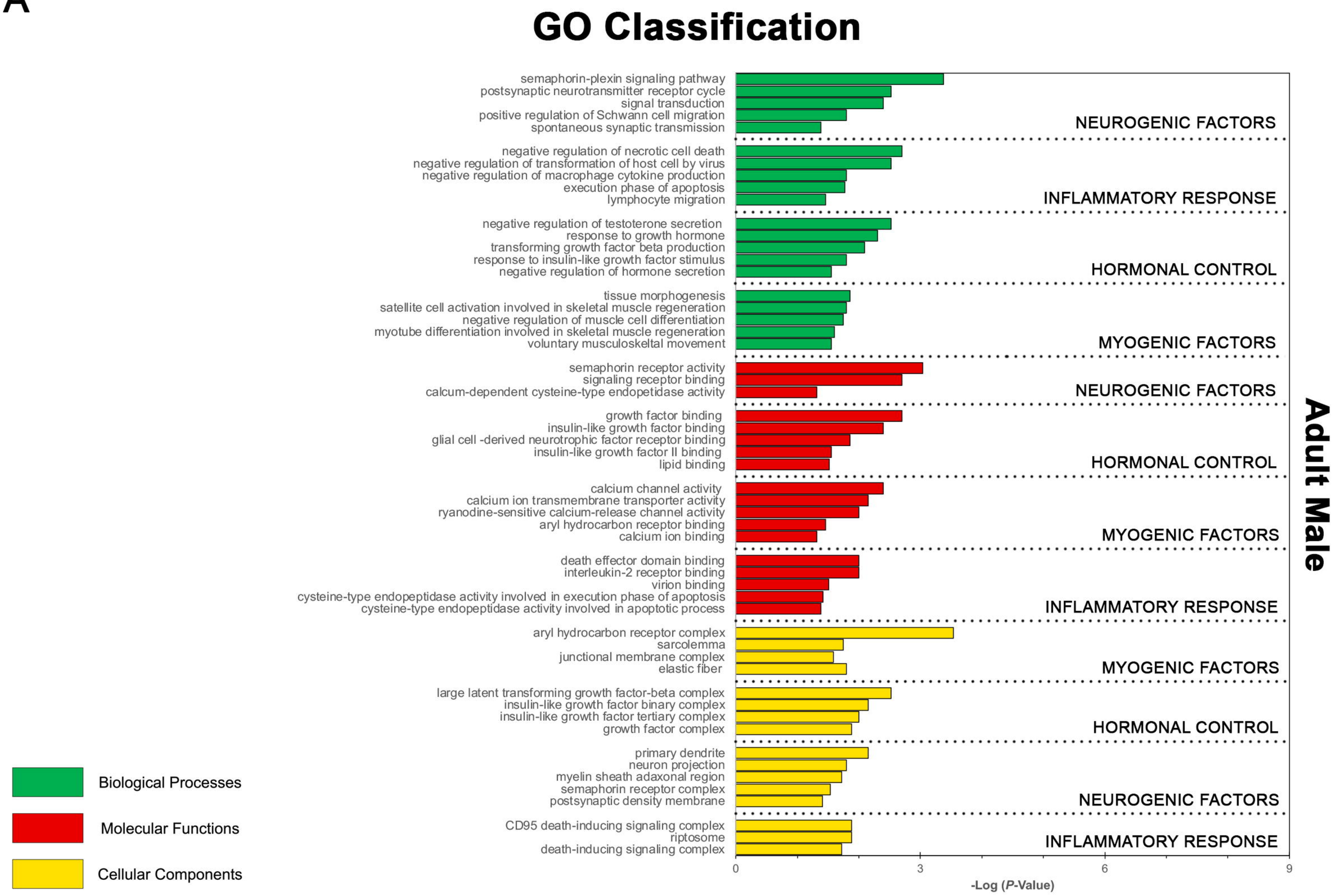
GO Classification
semaphorin-plexin signaling pathway
postsynaptic neurotransmitter receptor cycle
signal transduction
positive regulation of Schwann cell migration
spontaneous synaptic transmission
NEUROGENIC FACTORS
negative regulation of necrotic cell death
negative regulation of transformation of host cell by virus
negative regulation of macrophage cytokine production
execution phase of apoptosis
lymphocyte migration
INFLAMMATORY RESPONSE
negative regulation of testoterone secretion
response to growth hormone
transforming growth factor beta production
response to insulin-like growth factor stimulus
negative regulation of hormone secretion
HORMONAL CONTROL
tissue morphogenesis
satellite cell activation involved in skeletal muscle regeneration
negative regulation of muscle cell differentiation
myotube differentiation involved in skeletal muscle regeneration
voluntary musculoskeltal movement
MYOGENIC FACTORS
semaphorin receptor activity
signaling receptor binding
calcum-dependent cysteine-type endopetidase activity
NEUROGENIC FACTORS
growth factor binding
insulin-like growth factor binding
glial cell -derived neurotrophic factor receptor binding
insulin-like growth factor II binding
lipid binding
HORMONAL CONTROL
calcium channel activity
calcium ion transmembrane transporter activity
ryanodine-sensitive calcium-release channel activity
aryl hydrocarbon receptor binding
calcium ion binding
MYOGENIC FACTORS
death effector domain binding
interleukin-2 receptor binding
virion binding
cysteine-type endopeptidase activity involved in execution phase of apoptosis
cysteine-type endopeptidase activity involved in apoptotic process
INFLAMMATORY RESPONSE
aryl hydrocarbon receptor complex
sarcolemma
junctional membrane complex
elastic fiber
MYOGENIC FACTORS
large latent transforming growth factor-beta complex
insulin-like growth factor binary complex
insulin-like growth factor tertiary complex
growth factor complex
HORMONAL CONTROL
primary dendrite
neuron projection
myelin sheath adaxonal region
semaphorin receptor complex
postsynaptic density membrane
NEUROGENIC FACTORS
CD95 death-inducing signaling complex
riptosome
death-inducing signaling complex
INFLAMMATORY RESPONSE
0
3
6
9
-Log (P-Value)
Adult Male
Biological Processes
Molecular Functions
Cellular Components

B

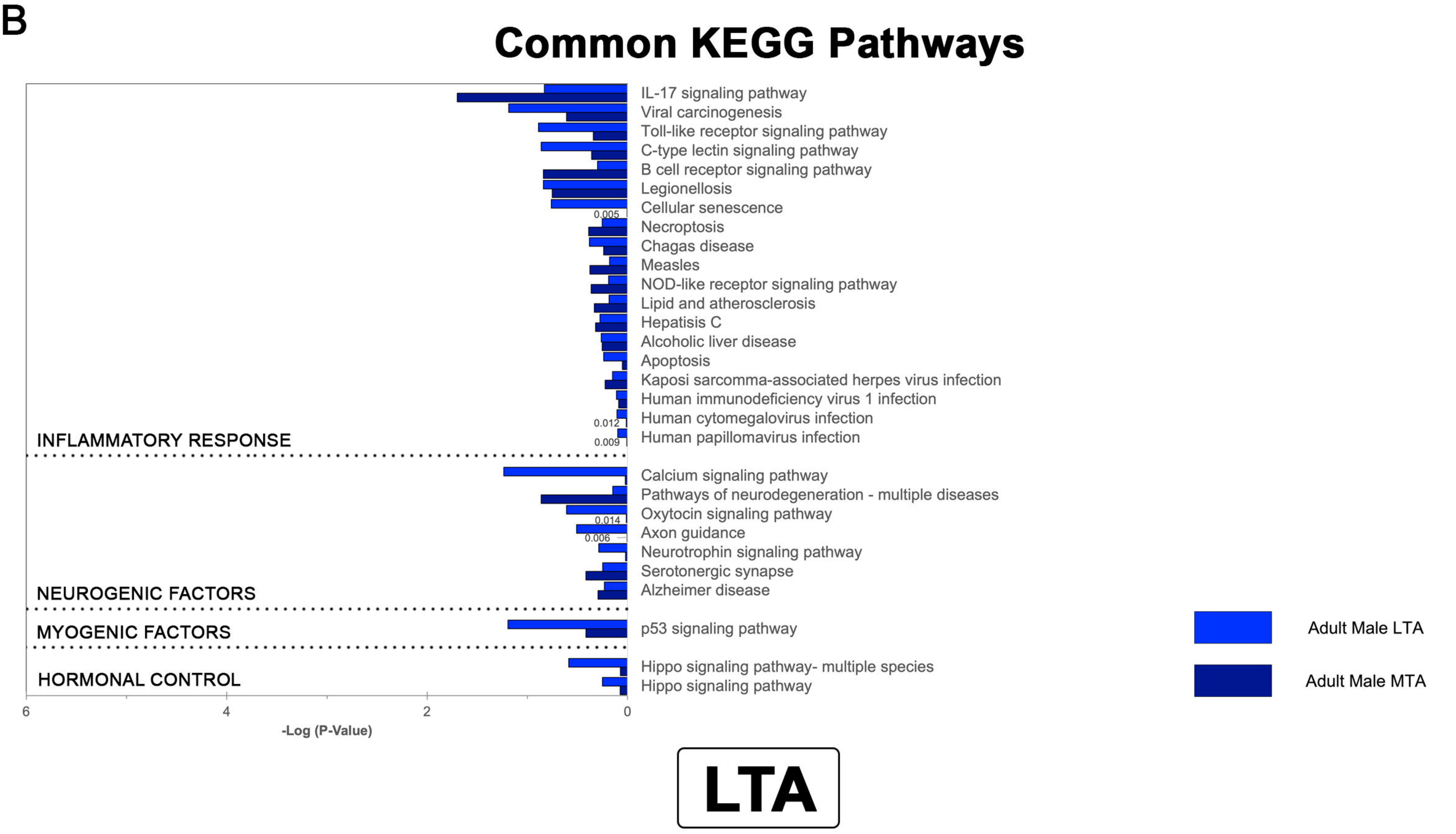
Common KEGG Pathways
IL-17 signaling pathway
Viral carcinogenesis
Toll-like receptor signaling pathway
C-type lectin signaling pathway
B cell receptor signaling pathway
Legionellosis
Cellular senescence
0.005
Necroptosis
Chagas disease
Measles
NOD-like receptor signaling pathway
Lipid and atherosclerosis
Hepatisis C
Alcoholic liver disease
Apoptosis
Kaposi sarcomma-associated herpes virus infection
Human immunodeficiency virus 1 infection
Human cytomegalovirus infection
0.012
0.009
Human papillomavirus infection
INFLAMMATORY RESPONSE
Calcium signaling pathway
Pathways of neurodegeneration - multiple diseases
Oxytocin signaling pathway
0.014
Axon guidance
0.006
Neurotrophin signaling pathway
Serotonergic synapse
Alzheimer disease
NEUROGENIC FACTORS
MYOGENIC FACTORS
p53 signaling pathway
HORMONAL CONTROL
Hippo signaling pathway- multiple species
Hippo signaling pathway
6
4
2
0
-Log (P-Value)
Adult Male LTA
Adult Male MTA

LTA

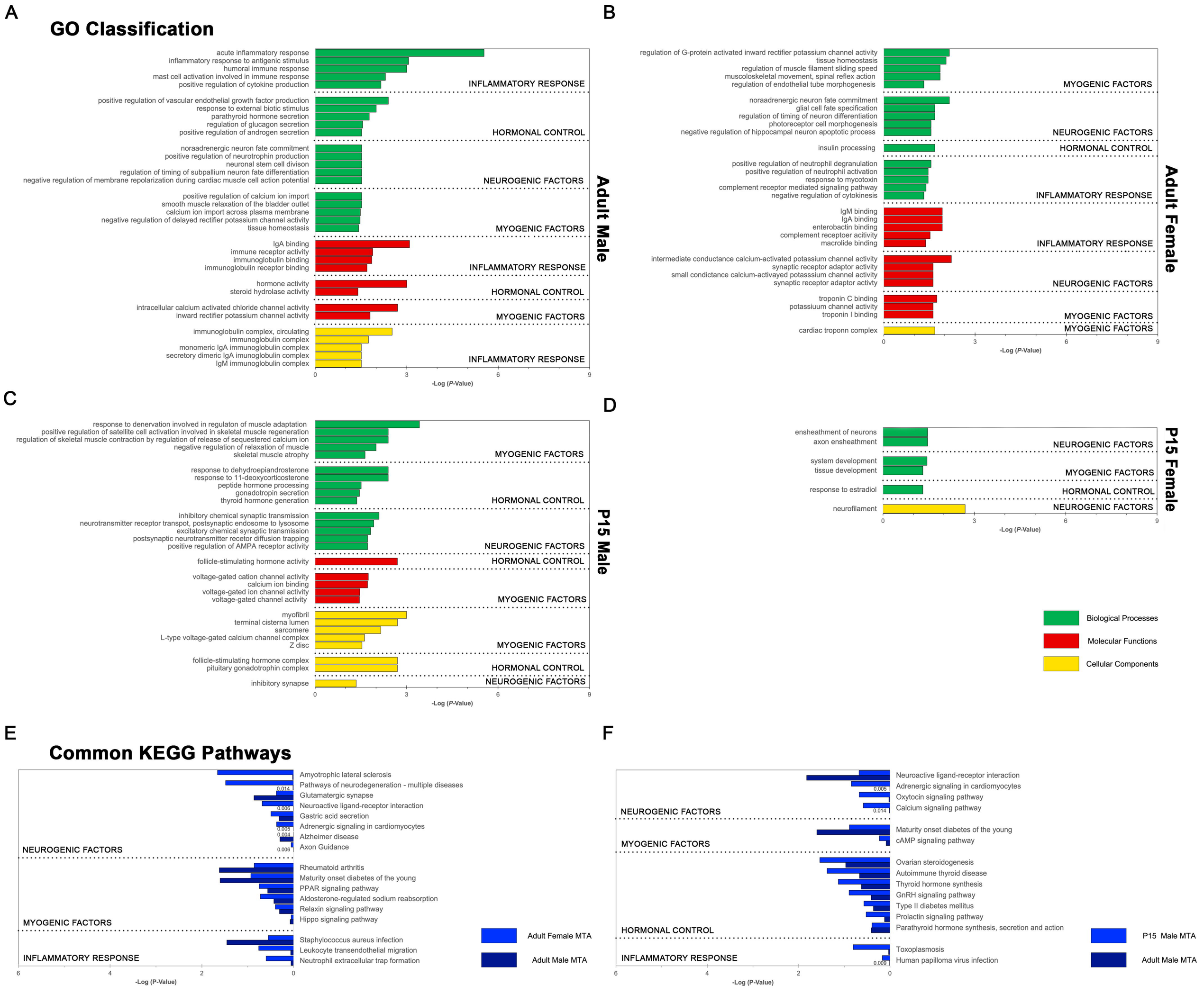
A
GO Classification
acute inflammatory response
inflammatory response to antigenic stimulus
humoral immune response
mast cell activation involved in immune response
positive regulation of cytokine production
INFLAMMATORY RESPONSE
positive regulation of vascular endothelial growth factor production
response to external biotic stimulus
parathyroid hormone secretion
regulation of glucagon secretion
positive regulation of androgen secretion
HORMONAL CONTROL
noraadrenergic neuron fate commitment
positive regulation of neurotrophin production
neuronal stem cell divison
regulation of timing of subpallium neuron fate differentiation
negative regulation of membrane repolarization during cardiac muscle cell action potential
NEUROGENIC FACTORS
positive regulation of calcium ion import
smooth muscle relaxation of the bladder outlet
calcium ion import across plasma membrane
negative regulation of delayed rectifier potassium channel activity
tissue homeostasis
MYOGENIC FACTORS
IgA binding
immune receptor activity
immunoglobulin binding
immunoglobulin receptor binding
INFLAMMATORY RESPONSE
hormone activity
steroid hydrolase activity
HORMONAL CONTROL
intracellular calcium activated chloride channel activity
inward rectifier potassium channel activity
MYOGENIC FACTORS
immunoglobulin complex, circulating
immunoglobulin complex
monomeric IgA immunoglobulin complex
secretory dimeric IgA imunoglobulin complex
IgM immunoglobulin complex
INFLAMMATORY RESPONSE
0
3
6
9
-Log (P-Value)
Adult Male
B
regulation of G-protein activated inward rectifier potassium channel activity
tissue homeostasis
regulation of muscle filament sliding speed
muscoloskeletal movement, spinal reflex action
regulation of endothelial tube morphogenesis
MYOGENIC FACTORS
noraadrenergic neuron fate commitment
glial cell fate specification
regulation of timing of neuron differentiation
photoreceptor cell morphogenesis
negative regulation of hippocampal neuron apoptotic process
NEUROGENIC FACTORS
insulin processing
HORMONAL CONTROL
positive regulation of neutrophil degranulation
positive regulation of neutrophil activation
response to mycotoxin
complement receptor mediated signaling pathway
negative regulation of cytokinesis
INFLAMMATORY RESPONSE
IgM binding
IgA binding
enterobactin binding
complement receptoer acitivity
macrolide binding
INFLAMMATORY RESPONSE
intermediate conductance calcium-activated potassium channel activity
synaptic receptor adaptor activity
small condictance calcium-activayed potasssium channel activity
synaptic receptor adaptor activty
NEUROGENIC FACTORS
troponin C binding
potassiuum channel activity
troponin I binding
MYOGENIC FACTORS
cardiac troponn complex
MYOGENIC FACTORS
0
3
6
9
-Log (P-Value)
Adult Female
C
response to denervation involved in regulaton of muscle adaptation
positive regulation of satellite cell activation involved in skeletal muscle regeneration
regulation of skeletal muscle contraction by regulation of release of sequestered calcium ion
negative regulation of relaxation of muscle
skeletal muscle atrophy
MYOGENIC FACTORS
response to dehydroepiandrosterone
response to 11-deoxycorticosterone
peptide hormone processing
gonadotropin secretion
thyroid hormone generation
HORMONAL CONTROL
inhibitory chemical synaptic transmission
neurotransmitter receptor transpot, postsynaptic endosome to lysosome
excitatory chemical synaptic transmission
postsynaptic neurotransmitter recetor diffusion trapping
positive regulation of AMPA receptor activity
NEUROGENIC FACTORS
follicle-stimulating hormone activity
HORMONAL CONTROL
voltage-gated cation channel activity
calcium ion binding
voltage-gated ion channel activity
voltage-gated channel activity
MYOGENIC FACTORS
myofibril
terminal cisterna lumen
sarcomere
L-type voltage-gated calcium channel complex
Z disc
MYOGENIC FACTORS
follicle-stimulating hormone complex
pituitary gonadotrophin complex
HORMONAL CONTROL
inhibitory synapse
NEUROGENIC FACTORS
0
3
6
9
-Log (P-Value)
P15 Male
D
ensheathment of neurons
axon ensheathment
NEUROGENIC FACTORS
system development
tissue development
MYOGENIC FACTORS
response to estradiol
HORMONAL CONTROL
neurofilament
NEUROGENIC FACTORS
0
3
6
9
-Log (P-Value)
P15 Female
Biological Processes
Molecular Functions
Cellular Components
E
Common KEGG Pathways
Amyotrophic lateral sclerosis
Pathways of neurodegeneration - multiple diseases
0.014
Glutamatergic synapse
0.006
Neuroactive ligand-receptor interaction
Gastric acid secretion
0.005
Adrenergic signaling in cardiomyocytes
0.004
Alzheimer disease
0.006
Axon Guidance
NEUROGENIC FACTORS
Rheumatoid arthritis
Maturity onset diabetes of the young
PPAR signaling pathway
Aldosterone-regulated sodium reabsorption
Relaxin signaling pathway
Hippo signaling pathway
MYOGENIC FACTORS
Staphylococcus aureus infection
Leukocyte transendothelial migration
Neutrophil extracellular trap formation
INFLAMMATORY RESPONSE
6
4
2
0
-Log (P-Value)
Adult Female MTA
Adult Male MTA
F
Neuroactive ligand-receptor interaction
Adrenergic signaling in cardiomyocytes
0.005
Oxytocin signaling pathway
Calcium signaling pathway
0.014
NEUROGENIC FACTORS
Maturity onset diabetes of the young
cAMP signaling pathway
MYOGENIC FACTORS
Ovarian steroidogenesis
Autoimmune thyroid disease
Thyroid hormone synthesis
GnRH signaling pathway
Type II diabetes mellitus
Prolactin signaling pathway
Parathyroid hormone synthesis, secretion and action
HORMONAL CONTROL
Toxoplasmosis
Human papilloma virus infection
0.009
INFLAMMATORY RESPONSE
6
4
2
0
-Log (P-Value)
P15 Male MTA
Adult Male MTA
MTA
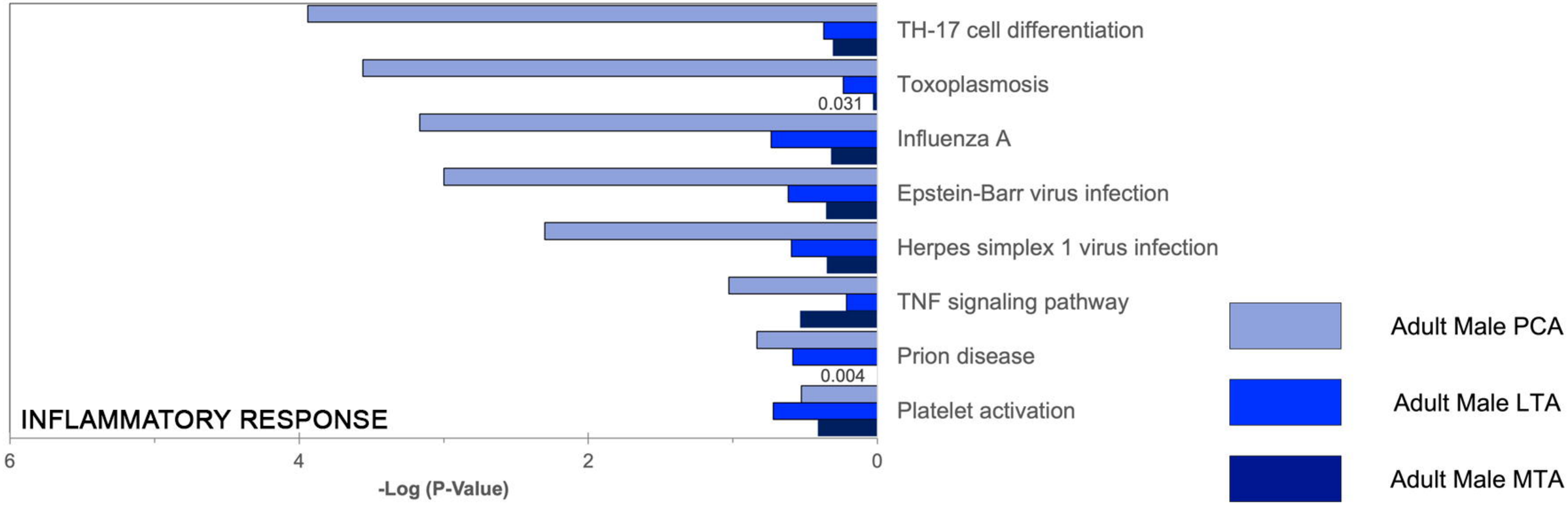
Common KEGG Pathways